



Vitreous collagen fragment dimensions after vitrectomy: a pilot study addressing the cut-rate enigma

Tommaso Rossi¹ · Alessio Bocedi² · Sara Notari² · Diego Sbardella¹ · Laura Fazi⁶ · Anna Priorello⁶ · Giorgio Querzoli³ · Sara Giammaria¹ · Gianmario Anselmi¹ · Mario R. Romano⁴ · Mattia Gianandrea Gaboardi⁶ · Giovanni Romanelli⁶ · Roberto Senesi⁶ · David H. Steel⁵ · Triestino Minniti⁶

Received: 11 October 2025 / Revised: 16 January 2026 / Accepted: 14 March 2026
© The Author(s) 2026

Abstract

Purpose to measure vitreous fragments generated at 5,000 and 20,000 cuts-per-minute (CPM) by means of Scanning Electronic Microscopy (SEM; fragments > 550 nm), Optical Profilometry and Dynamic Light Scattering (DLS; fragments 10–550 nm) and assess if cut-rate affects vitreous fragment size.

Methods Vitreous samples at 5k and 20 K CPM were collected from 3 patients undergoing 25G pars plana vitrectomy for macular pucker. SEM and Profilometry measured fragment size in 6 drops from each sample, DLS analysed the remainder. Each patient contributed 2 samples at 5 K and 20 K CPM taken at the beginning of surgery.

Results The median volume was 1,153.6 μm^3 (IQR 2,322.3 μm^3) at 5k and 72,4 μm^3 (IQR 923.4 μm^3) at 20k, respectively (Mann-Whitney $p=0.074$); the variability of vitreous fragment volume was higher for 5 K CPM group ($p=0.036$). DSL median fragment dimension in the 10–550 nm range was 50.7 nm (IQR 87.8 nm) for the 5 K CPM group and 43.8 nm (IQR 95.9 nm) for the 20 K CPM group ($p<0.001$).

Conclusion A fourfold increase in cut-rate did not produce significantly smaller vitreous fragments but the 20 K CPM samples showed less variability. Fragments size spanned 5 orders of magnitude (from nanometers to hundreds of microns), challenging the assumption that blade action produces uniform fragments. Fragment size variability minimally affected by cut-rate, questions the blade action as the main or only factor shearing vitreous. Elongation stress and shear stress most likely play a prominent role.

Key Messages

What is known

- Cut-rate of vitrectomy probes is regarded as the way to produce smaller vitreous fragments and reduce retinal traction.
- Higher cut-rates are considered safer for vitreous shaving.

What is new

- Vitreous fragments collected at 5,000 and 20,000 cuts per minute (CPM) did not show significantly different collagen fragment volumes as examined by Electron Microscopy.
- The dimension of collagen fragments ranged from nanometers to hundreds of microns in both the 5K and 20K CPM groups, despite blade motions cycling at millimetric distances.
- Shear and elongation stress may be responsible of collagen quaternary structure disruption more than the blade cutting action itself.

Keywords Pars plana vitrectomy · Cut rate · Vitreous fragments · Scanning electron microscopy · Dynamic light scattering · Collagen · Human vitreous · Optical profilometry

Extended author information available on the last page of the article

Introduction

Pars Plana Vitrectomy (PPV) is an effective treatment for complex retinal disorders, including rhegmatogenous retinal detachment [1], proliferative diabetic retinopathy, macular holes, and epiretinal membranes [2].

The human vitreous is a gel made of 98% water with a 3D mesh of collagen and interspersed hyaluronates and chondroitin sulphate [3]. The vitreous can be separated from the retina posteriorly, however, vitreous collagen fibrils insert into the retina at the vitreous base and in areas of abnormal vitreoretinal adhesion, where vitreoretinal separation can be difficult or impossible to create [4]. In these areas the vitreous must be cut and trimmed to the retina surface (so-called "shaving") to be safely removed.

Vitrectomy is accomplished through miniaturized handpieces with narrow bore cannulas housing guillotine cutters (23–27 gauge (G)) and typically operating at cut rates between 1,000 and 20,000 cuts per minute (CPM). Vitreous cutters are made of two coaxial hollow steel cylinders; the outer has a side port allowing vitreous inflow according to vacuum, and the inner cylinder acts as a blade sliding proximal-to-distal, severing the vitreous collagen fibrils.

The quest for higher cut-rates started with the very introduction of the VISC in 1975, to increase the reciprocation frequency and theoretically reduce the cut vitreous collagen fibre length and in turn retinal traction [5, 6]. This assumption has been challenged by Rossi et al. who described the extreme variability of both vitreous collagen fragments after vitrectomy using immune-blotting and -histochemistry as well as the instantaneous velocity at the cutter port, due to blade dragging and viscosity changes [7, 8].

Scanning Electron Microscopy with Energy Dispersive Spectroscopy (SEM/EDS) can accurately identify the atomic composition and measure vitreous collagen fragments [5]. The same vitreous collagen fragments analysed by SEM can also be analysed by optical profilometry to define their three-dimensional morphology. Dynamic Light Scattering (DLS) has also been applied to the human vitreous [6] and is used to infer the dimensions of generic light scattering particles ranging between 10 and 550 nm although it cannot distinguish their nature.

The purpose of the present study was to explore the effect of cut rate on vitreous fragment dimensions, using SEM/EDS, optical profilometry and DLS on vitreous samples collected at 5,000 and 20,000 CPM, representing two extreme cut rates of currently available systems.

Materials and methods

Pars plana vitrectomy

Vitreous samples from 3 patients undergoing 25G PPV for idiopathic macular pucker were collected using the R-Evolution CR 800 vitrectomy console with dual cutting action, 20 K CPM maximum cut-rate, pneumatic return (BVI, Waltham, USA) by a single surgeon (TR). The machine is equipped with a dual Venturi effect and peristaltic pump, but for this study, only the Venturi pump was used with fixed vacuum at 500 mmHg during sampling procedures.

Patients contributing specimens were 2 women and 1 man, age range 58–65 years; refraction was comprised between -1.25 and $+0.75$ in spherical equivalent. All patients were phakic and underwent an uneventful associated phacoemulsification and vitrectomy procedure with in-the-bag IOL implant. No patients had a relevant anamnesis for systemic illnesses with particular regard to connective tissue disease. No patients had associated ocular co-morbidities with special regard to glaucoma and *pseudoexfoliation* syndrome.

Each patient contributed two vitreous samples of about 1 cc each, taken at the beginning of the procedure, respectively at 5,000 CPM and 20,000 CPM, starting with the former. The vitreous specimens were collected after operating the cutter with the above settings for 30 s after which the probe was removed from the eye, the aspiration tubing disconnected about 15 centimetres proximal to the cutter probe and the vitreous filling the cutter shaft and distal tubing aspirated within 10 cc syringe and immediately stored at -80°C .

The vitreous cutter shaft and the entire aspiration line were thoroughly rinsed with 50+cc of Balanced Salt Solution (BSS) between samples, to flush vitreous remnants of the previous sampling and ensure there was no cross contamination between consecutive samples.

All patients were properly informed, accepted to participate to the study and signed appropriate and specific consent form. The study design followed the tenets of the Helsinki declaration and received Institutional Board approval (ERMLAB01 N° 77/18/FB).

Vitreous samples pre-treatment for SEM, profilometer and DLS samples

Before instrumental measurement, each sample underwent desalting and pre-concentration procedures through centrifugation at 14,000 rounds per minute for 10 min (Amicon Ultra; membrane cut-off 3 kDa MW; Merck Millipore,

Burlington, USA). The flow-through solutions were discarded, and the upper enriched fragments unfiltered portion was resuspended in ultrapure Mill-Q water.

Scanning electron microscopy (SEM), elemental composition of vitreous fragments and optical profilometry

Scanning electron microscopy with energy dispersive X-ray spectroscopy (SEM/EDS) combines the high-resolution images of surface topography with analysis of chemical elements and distribution in the observed objects.

Six drops of each sample were deposited on a silicon wafer for ten minutes at 20° until complete evaporation of the liquid phase occurred. The specimen was then mounted on a metal stub using a sticky carbon disc and then coated with gold applied in a sputter coater. The organic origin of all examined fragments was confirmed with EDS showing the combined presence of nitrogen, carbon and oxygen (Fig. 1).

Statistical analysis

Distributions of the volume and the Dynamic Light Scattering of the vitreous fragments were compared with non-parametric tests, as appropriate, after checking for normality with the Shapiro Wilk test. P value < 0.05 was considered

statistically significant. The statistical analysis was conducted with JASP Ver. 095 (The Netherlands).

After elemental validation, the same vitreous fragments identified with SEM, were analysed by Optical Profilometer (Zeta 20, KLA Instruments, Milpita, CA, USA) to assess their 3D shapes, roughness and volumes (Fig. 1b and c). Five vitreous fragments for each patient were identified and measured, totalling 15 specimens per cut-rate group.

Physical characterization of vitreous samples by dynamic light scattering (DLS)

Dynamic Light Scattering was used to determine the hydrodynamic diameter of fragments present in vitreous samples. The sample solutions of all patients, obtained after ultra-filtration were pooled and analysed in semi-micro-optical polystyrene cuvettes using a Zetasizer Nano ZS (Malvern Panalytical, Malvern, UK). Each measurement was subtracted by the signal of water impurities and performed with the following setting panel: 20 accumulations, water as dispersant, temperature of 25 °C, and 120 s of equilibration time. DLS data acquisition and the selection and validation of particle size distributions for each sample were performed by ZS XPLOER software (Malvern Panalytical, Malvern, GB). A dimension of less than 550 nm is considered the reliability threshold.

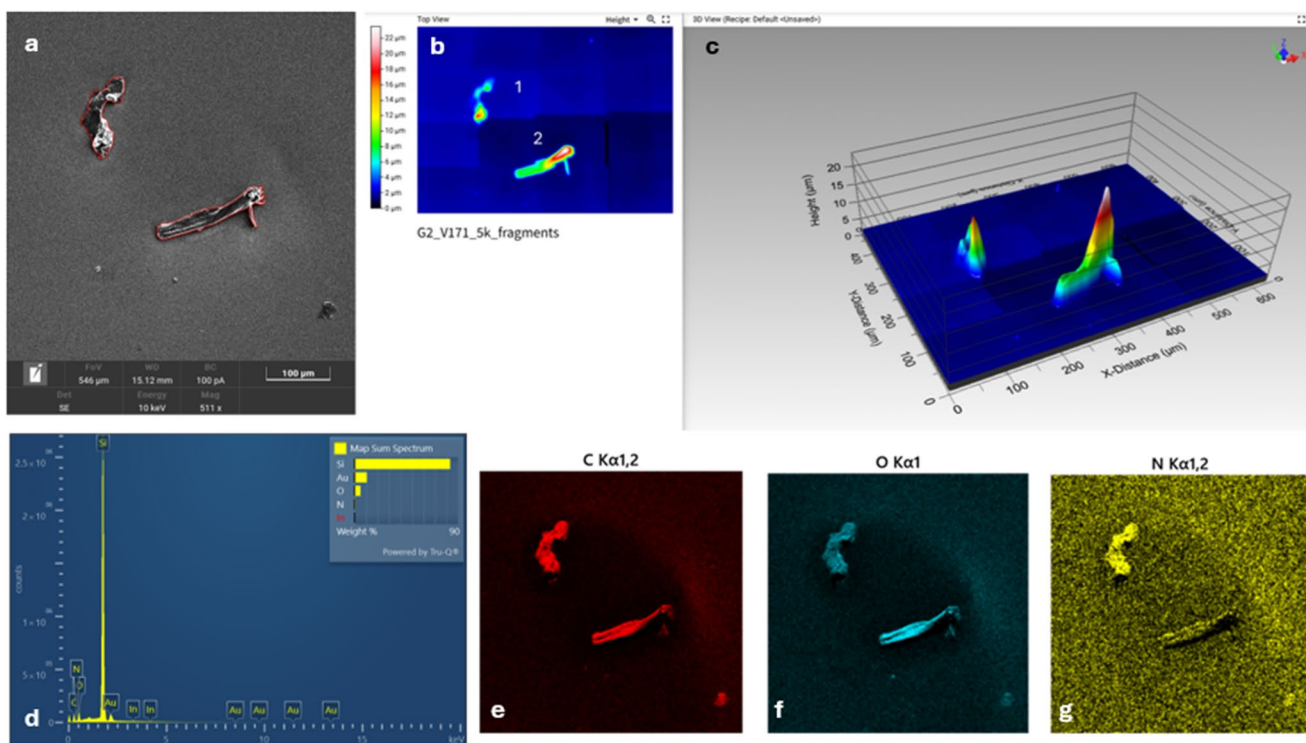


Fig. 1 **a)** Scanning Electron Microscopy of vitreous fragments. **b)** and **c)** 2D and 3D Profilometer image; **d)** SEM/EDS spectrum shows the elemental composition of the analysed sample, confirming the pres-

ence of carbon (C), nitrogen (N), oxygen (O), together with wafer Silicon and coating gold; **e),f),g)** Same image as **a)** with red, blue and yellow spectra assigned to C, O and N, respectively

Results

The median volume of vitreous fragments examined by SEM, validated by SEM/EDS and acquired by an Optical Profilometer, was 1,153.6 (InterQuartile Range; IQR 2,322.3) μm^3 at 5 K CPM and 72.4 (IQR 923.4) μm^3 at 20 K CPM respectively. Data were not normally distributed (Shapiro-Wilk test $p < 0.001$). The volume of vitreous fragments taken at 5 K CPM was not significantly different from those collected at 20 K CPM (Mann-Whitney $p = 0.074$; Mood's test $p = 0.699$). Both cut-rates generated fragments ranging from nanometres to over 200 microns. The dispersion of vitreous fragments volume was significantly higher for 5 K CPM compared to 20 K CPM cut-rate (Levene's test $p = 0.036$).

Dynamic Light Scattering of vitreous fragments comprised between 10 and 550 nm (Fig. 2) showed a non-normal distribution of both datasets (Shapiro-Wilk Test $p < 0.01$). There were negligible but statistically significant differences between the 5 K and 20 K CPM groups in terms of their respective intensity curve distribution (Fig. 2a; 2-Sample) with median values of 50.7 nm (IQR 87.8) for the 5 K CPM group and 43.8 nm (IQR 82.5) for the 20 K CPM group (Mann-Whitney test $p < 0.001$).

Discussion

Since the introduction of PPV, cut rates have steadily increased as manufacturers improved blade driving technologies introducing dual action cutting [8]. Raising cut-rate is technologically demanding and expensive; therefore, investigating the effects of cut rate may help manufacturers focus on relevant future development strategies.

The rationale behind the relentless increase in cut rates, relies on the assumption that higher cutting frequencies

reduce traction exerted by vitreous fibers on the retina [9]; an axiom supported by experimental evidence with single action guillotine probes [10] (increasingly redundant now), but never unequivocally proven for dual-action cutting probes with a near 100% open duty cycle [11].

Interestingly, previous studies failed to prove a significant difference in the average vitreous fragments' dimensions when samples were collected at cut rates varying from 1,000 CPM to 16,000 CPM and analyzed with different methods, including Western Blot [10] and immuno-histochemistry [8]. In neither case was a satisfying explanation reached and the erratic fluid velocity at the cutter port, resulting in flow rate variability [9] was hypothesized as a possible factor. Those studies also suffered from limitations inherent to the chosen methods since both the processing necessary for Western Blot and the ligand site for immunochemistry may have had limited sensitivity and/or specificity.

The present study using SEM/EDS, Profilometry and DLS, offered the advantage of confirmation of the specimen atomic composition and direct vitreous fragments visualization and measurement. The median fragment size of samples collected at opposite sides of the cut rate spectrum (5 K and 20 K CPM) yielded statistically significant but clinically negligible differences only for smaller fragments between 10 and 550 nm and no difference for larger fragments. In other words, quadrupling the cut rate did not produce smaller collagen fragments overall, although it did reduce their variability.

Even more interestingly, the study showed that cutting at either 5–20 K CPM produced a myriad of fragments spanning 5 orders of magnitude in size, from nanometers to hundreds of microns: a conundrum deserving further scrutiny.

In principle, the dimension of vitreous fragments depends on the cut-rate and the flowrate, i.e. it is proportional to the distance travelled by the vitreous through the port between two consecutive cuts (Fig. 3; see Appendix A). The

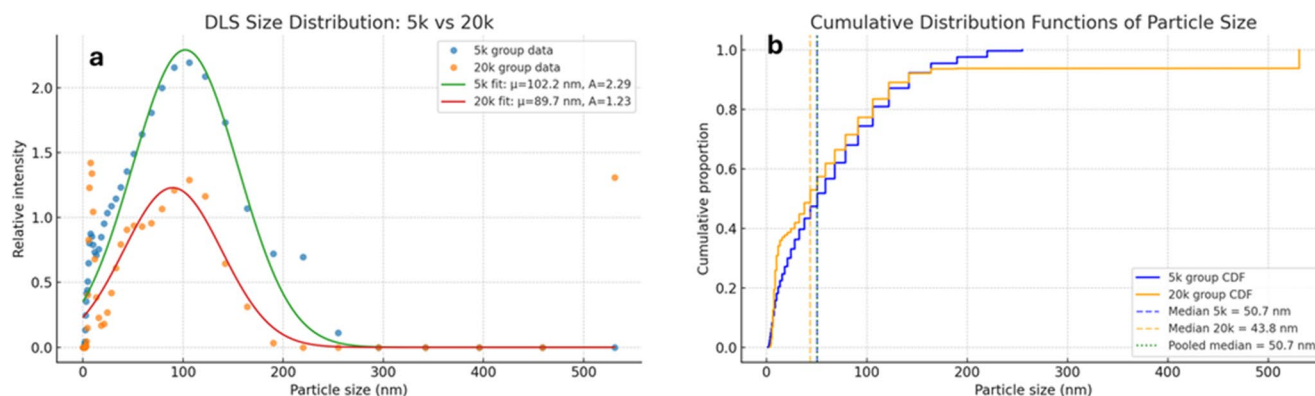


Fig. 2 a) Dynamic Light Scattering weighted intensity (%) of vitreous fragments within the 10–500 nm range, collected at 5 K and 20 K CPM. **b)** Cumulative distribution functions for 5K and 20K groups

show a slightly greater representation of fragments under 50 microns for the 20 K group (yellow line) compared to the 5 K group (blue line)

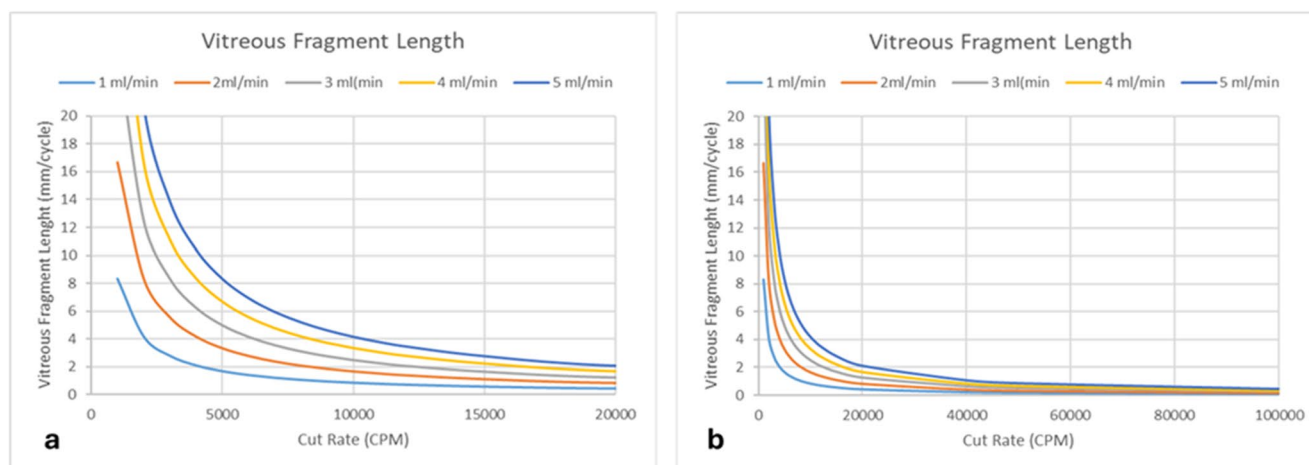


Fig. 3 Distance travelled by an ideal vitreous element between two consecutive cuts (mm per cycle) as a function of cut-rate at steady flow rates ranging from 1 to 5 ml/min. **a)** between 5,000–20,000 CPM; **b)** extrapolated up to 100,000 CPM

evolution of vitreous cutter handpieces has to date, focused entirely on cutting mechanics, almost disregarding fluidics, despite experimental evidence showing a wide variability of the instantaneous flow rate at the cutter port [12]. This neglected flow instability may indeed nullify the advantages of higher cut-rates and the oversimplified assumption that the increase in cut rate will ease vitreous removal and reduce traction per se [11].

The largest fragments identified by SEM for both 5 K and 20 K CPM groups, were in the order of tens to hundreds of microns (Fig. 4). Then, how can a blade that is cycling at millimetric distances (see Appendix A and Fig. 4) produce fragments in the nanometer to micrometer range? And why is there such a variability regardless of cut rate?

The vitreous gel is made of 98% water with interspersed proteoglycans, hyaluronate, and collagen fibers, which is the only structure requiring cutting to be excised. If blade motion were the prevailing action in vitreous collagen excision, one would expect fragment size in the order of magnitude of millimeters created between two consecutive blade actions (Fig. 3) with some tolerance due to flow rate fluctuations related to dragging [9]. Our results highlight a completely different scenario: collagen fragments ranging from nanometers to hundreds of microns and seem minimally, if at all, affected by cut rates.

The present results suggest that, when the vitreous column is drawn into the cutter port by vacuum, the collagen mesh (actually its quaternary proteic structure) is torn apart and randomly shredded by a combination of forces including the high extensional and shear stress due to the combined action of chaotic fluid motion through variations in the cross sectional area of the port zone (port versus inner lumen and moving blade), high velocity (over 1 m/s), acceleration (over 400 m/s^2) [13], and also blade motion itself, rather than being consistently cut by the blade, as if it were

some dough pushed through a die cast. It is therefore conceivable that all the above mechanisms concur to vitreous collagen shredding and contribute with fragments of diverse dimension.

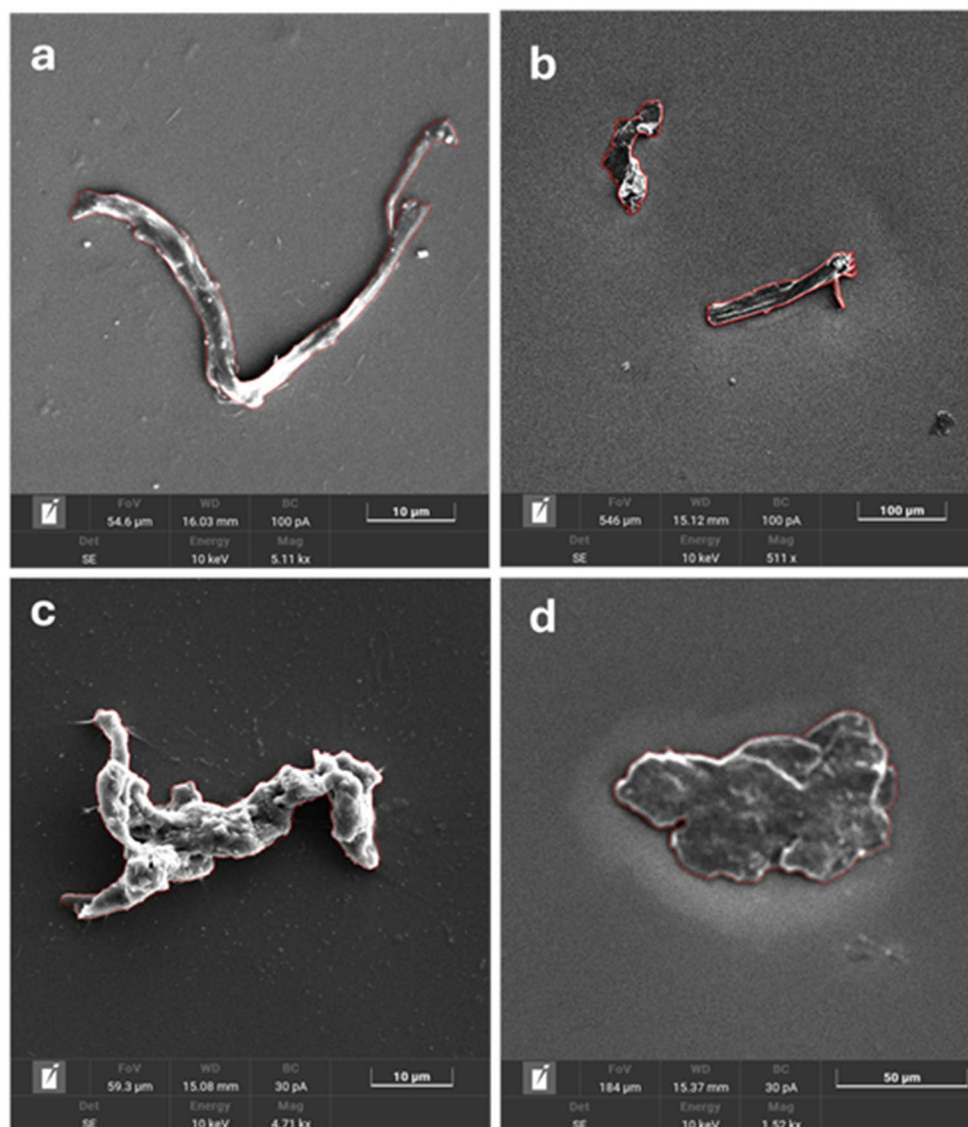
This explanation concurs with the fact that increasing the cut rate did not translate into an appreciable decrease in fragment size, but only in a modest (though significant) reduction of their variability. Whether this result is surgically valuable and decreases the tractional forces transmitted to the retina, thus increasing the safety of the procedure, is debatable.

Then, if the blade is not just severing vitreous chunks into consecutive identical pieces, what is its role, and how does it affect fragment dimensions? Most likely, a higher frequency engages smaller discrete volumes of vitreous into the port, severing their distal attachment and minimizing inadvertent surgical traction by probe movement. It also adds shear stress to collagen molecules as they slide across the port, favoring the progression of vitreous through the probe and possibly prompting the cascade of events previously hypothesized [14].

On the other hand, it should also be noted that increasing cut rate also produces undesired effects like a pulsatile flow alternatively moving in opposite directions, generating repulsion and opposing aspiration. Furthermore, if the fragment size simply adhered to the ideal dimensions depicted in Fig. 3, a strategy directed to the asymptotic increase of cut rate would yield limited advantage, at the cost of increasing technical complexity.

In summary, despite suffering from limitations, including the relative paucity of samples, the possible coiling, aggregation or modifications of vitreous strands due to SEM processing, our study shows a macroscopic mismatch between cut rate and fragment dimensions. It highlights the inefficiency of cut-rate increase as the only, or primary measure

Fig. 4 Examples of Scanning Electron Microscope images of vitreous fragments collected at 5K cut-rate (**a, b**) and 20K cut-rate (**c** and **d**). Note the different magnifications indicated by the segment in the right inferior corner of each image



aimed at reducing fragment size and warrants further study on a much larger scale.

The small sample size in the presence of the high variability observed may have resulted in the non-significant difference in fragment volume found between cut rates. Nonetheless, the wide variability in fragment size equally represented in both groups, is undoubtedly present and possibly represents the most interesting finding of this pilot study. This finding clearly challenges the established dogma that the blade is the main agent responsible for collagen disruption and introduces the hypothesis that extensional and shear stress may be viable alternative explanations.

The development of next generation vitreous cutters must pursue innovative approaches and reconsider many of today's undisputed beliefs, including reciprocation and blade action and explore macromolecular fluidics at least as much as mechanics.

Appendix

The 25G cutter has a nominal outer diameter of 0.51mm and inner diameter of 0.31, considering steel thickness about 0.1 mm. The cross-section is $A = \pi r^2 7.5 \times 10^{-8} \text{ m}^2$.

Velocity within the cutter is $v = \frac{Q}{A}$ where Q is flow and A is the above cross-section. Fragment length per cycle (distance fluid advances between two blade closures at cut rate f is: $L = \frac{Q}{Af}$ where L is the fragment length, Q is flowrate, A is cross section and f is the cut-rate.

Once all data are in the International Standard the curves for $Q = 1$ to 5 ml/min can be calculated and drawn as in figure 4.

Acknowledgements The authors would like to thank the “Fondazione Roma” and the Italian Ministry of Health for financial support. The authors gratefully acknowledge the support of the ISIS@MACH ITALIA Research Infrastructure, the hub of ISIS Neutron and Muon

Source (UK), [MUR official registry U. 0008642.28-05-2020–16th April 2020]. IM@IT is listed in the Italian Ministry of University and Research's Piano Nazionale delle Infrastrutture di Ricerca (PNIR 2021–2027) “in the broader notion of ISIS”, and ISIS Facility and IM@IT are jointly listed in high priority RI's.

Author contributions TR TM AB and GQ designed the study, wrote manuscript MRR DS GA revised the manuscript performed surgery and supervised data management SG DS revised the manuscript and carried out all statistics SN AP LF performed SEM analysis and profilometry MGG GR RS performed DLS analysis.

Data availability Data is provided within the manuscript or supplementary information files.

Declarations

Compliance with ethical standards No funding was received for this research and none of the authors has any conflict of interest to declare.

Financial disclosure None of the authors has any competing or conflict of interest related to the subject matter. No funding was involved in this study.

Competing interests The authors declare no competing interests.

Clinical trial number Not applicable.

Open Access This article is licensed under a Creative Commons Attribution-NonCommercial-NoDerivatives 4.0 International License, which permits any non-commercial use, sharing, distribution and reproduction in any medium or format, as long as you give appropriate credit to the original author(s) and the source, provide a link to the Creative Commons licence, and indicate if you modified the licensed material. You do not have permission under this licence to share adapted material derived from this article or parts of it. The images or other third party material in this article are included in the article's Creative Commons licence, unless indicated otherwise in a credit line to the material. If material is not included in the article's Creative Commons licence and your intended use is not permitted by statutory regulation or exceeds the permitted use, you will need to obtain permission directly from the copyright holder. To view a copy of this licence, visit <http://creativecommons.org/licenses/by-nc-nd/4.0/>.

References

1. Popovic MM, Muni RH, Nichani P, Kertes PJ (2022) Pars plana vitrectomy, scleral buckle, and pneumatic retinopexy for the management of rhegmatogenous retinal detachment: a meta-analysis. *Surv Ophthalmol* 67(1):184–196. <https://doi.org/10.1016/j.survophthal.2021.05.008>

2. Mihalache A, Huang RS, Ahmed H, Patil NS, Popovic MM, Kertes PJ, Muni RH (2024) Pars plana vitrectomy with or without internal limiting membrane peel for epiretinal membrane: a systematic review and meta-analysis. *Ophthalmologica* 247(1):30–43. <https://doi.org/10.1159/000534851>
3. Ayalon A, Sahel JA, Chhablani J (2024) A journey through the world of vitreous. *Surv Ophthalmol* 69(6):957–966. <https://doi.org/10.1016/j.survophthal.2024.06.004>
4. Inoue M, Koto T, Hirakata A (2021) FLOW DYNAMICS OF BEVELED-TIP AND FLAT-TIP VITREOUS CUTTERS. *Retina* 41(2):445–453. <https://doi.org/10.1097/IAE.0000000000002811>
5. Tamura T, Kishi S (1993) [Scanning electron microscopic findings of the premacular vitreous in eyes without posterior vitreous detachment]. *Nippon Ganka Gakkai zasshi* 97(10):1197–1202 Japanese. PMID: 7504879
6. Bettelheim FA, Zigler JS Jr. (2004) Regional mapping of molecular components of human liquid vitreous by dynamic light scattering. *Exp Eye Res* 79(5):713–8. <https://doi.org/10.1016/j.exer.2004.07.011>
7. Rossi T, Querzoli G, Angelini G, Malvasi C, Rossi A, Morini M, Esposito G, Micera A, di Luca NM, Ripandelli G (2016) Hydraulic resistance of vitreous cutters: the impact of blade design and cut rate. *Transl Vis Sci Technol* 5(4):1. <https://doi.org/10.1167/tvst.5.4.1>
8. Rossi T, Querzoli G, Malvasi C, Iossa M, Angelini G, Ripandelli G (2014) A new vitreous cutter blade engineered for constant flow vitrectomy. *Retina* 34(7):1487–91. <https://doi.org/10.1097/IAE.0000000000000251>
9. Steel DH, Charles S (2011) Vitrectomy fluidics. *Ophthalmologica* 226(1):27–35. <https://doi.org/10.1159/000328207>
10. Teixeira A, Chong L, Matsuoka N, Rowley A, Lue JC, McCormick M, Kerns R, Humayun M (2010) Novel method to quantify traction in a vitrectomy procedure. *Br J Ophthalmol* 94(9):1226–9. <https://doi.org/10.1136/bjo.2009.166637>
11. Steel DH, Charles M, Zhu Y, Tambat S, Irannejad AM, Charles S (2022) Fluidic performance of a dual-action vitrectomy probe compared with a single-action probe. *Retina* 42(11):2150–2158. <https://doi.org/10.1097/IAE.0000000000003573>
12. Rossi T, Querzoli G, Angelini G, Malvasi C, Rossi A, Morini M, Esposito G, Micera A, di Luca NM, Ripandelli G (2016) Hydraulic resistance of vitreous cutters: the impact of blade design and cut rate. *Transl Vis Sci Technol* 5(4):1. <https://doi.org/10.1167/tvst.5.4.1>
13. Veerasamy D, Vedeniapina D, Wilkes M, Steel DH, Whalley RD (2025) Characterizing the field of fluidic effect around vitrectomy probes using particle image velocimetry. *Transl Vis Sci Technol* 14(4):20. <https://doi.org/10.1167/tvst.14.4.20>
14. Sharif-Kashani P, Nishida K, Pirouz Kavehpour H, Schwartz SD, Hubschman JP (2013) Effect of cut rates on fluidic behavior of chopped vitreous. *Retina* 33(1):166–9. <https://doi.org/10.1097/IAE.0b013e31825db758>

Publisher's note Springer Nature remains neutral with regard to jurisdictional claims in published maps and institutional affiliations.

Authors and Affiliations

Tommaso Rossi¹ · Alessio Bocedi² · Sara Notari² · Diego Sbardella¹ · Laura Fazi⁶ · Anna Priorello⁶ · Giorgio Querzoli³ · Sara Giammaria¹ · Gianmario Anselmi¹ · Mario R. Romano⁴ · Mattia Gianandrea Gaboardi⁶ · Giovanni Romanelli⁶ · Roberto Senesi⁶ · David H. Steel⁵ · Triestino Minniti⁶

✉ Tommaso Rossi
tommaso.rossi@usa.net

¹ IRCCS Fondazione Bietti ONLUS, Via Livenza 3,
Roma 00198, Italy

² Department of Chemical Science and Technologies
Department of Chemical Science and Technologies,
University of Rome Tor Vergata, Roma, Italy

³ DICAAR Università degli Studi di Cagliari – Cagliari,
Cagliari, Italy

⁴ Department of Biomedical Science, Humanitas University,
Milano, Italy

⁵ Bioscience Institute, Newcastle University, Newcastle Upon
Tyne and Sunderland Eye Infirmary, Sunderland, UK

⁶ Department of Physics, Università degli Studi di Roma Tor
Vergata, Roma, Italy